Molecular Plant
Research Article

CellPress
PARTNER JOURNAL

Phosphorylation of Serine 186 of bHLH Transcription Factor SPEECHLESS Promotes Stomatal Development in *Arabidopsis*

Ke-Zhen Yang[1], Min Jiang[1], Ming Wang[1], Shan Xue[1], Ling-Ling Zhu[1], Hong-Zhe Wang[1], Jun-Jie Zou[1], Eun-Kyoung Lee[2], Fred Sack[2] and Jie Le[1,*]

[1]Key Laboratory of Plant Molecular Physiology, Institute of Botany, Chinese Academy of Sciences, 20 Nanxincun, Beijing 100093, China

[2]Department of Botany, University of British Columbia, Vancouver, British Columbia V6T 1Z4, Canada

***Correspondence: Jie Le (lejie@ibcas.ac.cn)**

http://dx.doi.org/10.1016/j.molp.2014.12.014

ABSTRACT

The initiation of stomatal lineage and subsequent asymmetric divisions in *Arabidopsis* require the activity of the basic helix-loop-helix transcription factor SPEECHLESS (SPCH). It has been shown that SPCH controls entry into the stomatal lineage as a substrate either of the MITOGEN-ACTIVATED PROTEIN KINASE (MAPK) cascade or GSK3-like kinase BRASSINOSTEROID INSENSITIVE 2 (BIN2). Here we show that three serine residues of SPCH appear to be the primary phosphorylation targets of Cyclin-Dependent Kinases A;1 (CDKA;1) *in vitro*, and among them Serine 186 plays a crucial role in stomatal formation. Expression of an *SPCH* construct harboring a mutation that results in phosphorylation deficiencies on Serine 186 residue failed to rescue stomatal defects in *spch* null mutants. Expression of a phosphorylation-mimic mutant *SPCH*^{S186D} complemented stomatal production defects in the transgenic lines harboring the targeted expression of dominant-negative *CDKA;1.N146*. Therefore, in addition to MAPK- and BIN2-mediated phosphorylation on SPCH, phosphorylation at Serine 186 is positively required for SPCH function in regulating stomatal development.

Key words: *Arabidopsis*, stomata, development, transcription factor, phosphorylation

Yang K.-Z., Jiang M., Wang M., Xue S., Zhu L.-L., Wang H.-Z., Zou J.-J., Lee E.-K., Sack F., and Le J. (2015). Phosphorylation of Serine 186 of bHLH Transcription Factor SPEECHLESS Promotes Stomatal Development in *Arabidopsis*. Mol. Plant. **8**, 783–795.

INTRODUCTION

Stomata are plant-specific epidermal structures required for CO_2 assimilation in photosynthesis as well as for evaporative cooling and water uptake (Casson and Hetherington, 2010). *Arabidopsis* stomata develop from young epidermal cells after two types of divisions, asymmetric and symmetric. The cell type that initiates the stomatal lineage, the Meristemoid Mother Cell (MMC), divides unequally producing a smaller, and often triangular, meristemoid (M), as well as a larger sister cell. Meristemoids typically undergo one to three rounds of amplifying divisions before forming a Guard Mother Cell (GMC). The larger sister cell can also divide unequally, divisions which are usually oriented so that the new stoma does not directly contact pre-existing ones. The symmetric division of the GMC generates a pair of young Guard Cells (GCs) that then undergo pore formation and stomatal morphogenesis (Nadeau and Sack, 2002a; Bergmann and Sack, 2007).

Arabidopsis stomatal development involves the secreted peptide ligands such as EPIDERMAL PATERNING FACTORS (i.e. EPF1, EPF2, STOMAGEN, CHALLAH), as well as signals received by TOO MANY MOUTHS (TMM) and the ERECTA family of receptors (Nadeau, 2009; Lau and Bergmann, 2012). These signals are in turn transduced via a mitogen-activated protein kinase (MAPK) cascade, which includes YODA (YDA), MKK4/5/7/9, and MPK3/6 (Bergmann et al., 2004; Wang et al., 2007). For example, the loss of *TMM* or *YODA* function results in the production of excess stomata in contact. Three basic helix-loop-helix (bHLH) transcription factors, SPEECHLESS (SPCH), MUTE, and FAMA, are required for successive stages of development including lineage initiation and proliferation, as well as terminal differentiation (Ohashi-Ito and Bergmann, 2006; MacAlister et al., 2007; Pillitteri et al., 2007). The R2R3-MYB transcription factors

Published by the Molecular Plant Shanghai Editorial Office in association with Cell Press, an imprint of Elsevier Inc., on behalf of CSPB and IPPE, SIBS, CAS.

FOUR LIPS (FLP) and MYB88 are also required to limit GMC symmetric divisions to one (Lai et al., 2005). The INDUCER OF CBF EXPRESSION 1 (ICE1)/SCREAM (SCRM), which regulates freezing tolerance, as well as SCRM2, are required for the functions of SPCH, MUTE, and FAMA at successive fate transitions during stomatal development (Kanaoka et al., 2008).

SPCH can be phosphorylated *in vitro* by MPK3 or MPK6. Constitutive expression of a mutated *SPCH* with a deleted MAPK target domain (MPKTD) induces the formation of excess stomata (Lampard et al., 2008). The phytohormone brassinosteroid (BR) regulates stomatal production via BIN2-mediated phosphorylation (Gudesblat et al., 2012; Kim et al., 2012; Khan et al., 2013). The serine/threonine glycogen synthase kinase 3 (GSK3)/SHAGGY-like BRASSINOSTEROID INSENSITIVE 2 (BIN2) phosphorylates YDA as well as the substrates of YDA, MKK4, and MKK5, resulting in lowered MPK3/6 activity in an MAPK module (Kim et al., 2012; Khan et al., 2013). MAPK- or BIN2-mediated phosphorylation leads to reduced SPCH activity or the degradation of the SPCH protein and, thus, suppressed stomatal development (Lampard et al., 2008; Gudesblat et al., 2012).

Cell-cycle genes play important roles in controlling cell division and differentiation during stomatal development. The *Arabidopsis* genome harbors 29 CYCLIN-DEPENDENT KINASEs (CDKs), which are subdivided into eight groups (CDKA to CDKG and CKL) (Menges et al., 2005). Abnormal single guard cells form when the function of both CDKB1;1 and CDKB1;2 are lost in *cdkb1;1 1;2* double mutants, as well as when a dominant-negative form of *CDKB1;1* (*35S:CDKB1;1.N161*) is constitutively expressed (Boudolf et al., 2004; Xie et al., 2010). *CDKA;1*, formerly known as *CDC2A*, is required for many aspects of plant development. Mutation in *CDKA;1* arrests or delays the second mitotic division during pollen development, resulting in seed abortion (Iwakawa et al., 2006; Nowack et al., 2006). Homozygous *cdka;1* mutants and transgenic lines expressing a dominant-negative *CDKA;1.N146* construct exhibit defects in embryogenesis and in maintenance of root and shoot apical meristems (Gaamouche et al., 2010; Nowack et al., 2012). The loss of *CDKA;1* function was shown to lead to defects in both initiation and terminal GMC divisions during stomatal development (Weimer et al., 2012; Yang et al., 2014). RETINOBLASTOMA-RELATED (RBR) is a homolog of the human tumor suppressor *Retinoblastoma* gene, which is phosphorylated predominantly by CDK kinases, such as CDKA;1 and CDKB1 (Nowack et al., 2012). Since chromatin immunoprecipitation (ChIP) PCR results indicate that RBR binds to the *SPCH* promoter, the function of CDKA;1 in asymmetric divisions was proposed to operate via the transcriptional regulation of *RBR* on *SPCH* (Weimer et al., 2012).

Here we show that, in addition to the previously described function of MAPK and BIN2 phosphorylation target sites, phosphorylation at the Serine 186 residue of SPCH is also critical for modulating SPCH function in stomatal development. Moreover, Serine186 of SPCH appears to be the primary phosphorylation target site of CDK *in vitro* and *in planta*. These findings reveal an additional mechanism that fine tunes SPCH activity and stability via phosphorylation by multiple kinases in regulating stomatal production.

RESULTS

Recovery of Homozygous *cdka;1* Seedlings

Since the second mitosis in pollen development is absent from about 50% of all pollen in *cdka;1*$^{+/-}$ heterozygotes, pollen grains contain just two nuclei rather than three, one vegetative and one sperm-like (Supplemental Figure 1A). As a result, about half of all seeds abort in *cdka;1*$^{+/-}$ siliques (Supplemental Figure 1F), so that no homozygous *cdka;1*$^{-/-}$ seeds are produced in self-pollinated *cdka;1*$^{+/-}$ plants (Iwakawa et al., 2006). To recover homozygous *cdka;1* mutant seedlings, *cdka;1*$^{+/-}$ plants (SALK_106809) were transformed with a *LAT52pro:CDKA;1* construct in which a full-length *CDKA;1* cDNA was fused to the pollen-specific promoter *LAT52* (Muschietti et al., 1994). More than 20 independent *cdka;1*$^{+/-}$ transgenic T_1 lines were obtained. T_2 plants included tiny seedlings with retarded root growth, short hypocotyls, and small cotyledons (Supplemental Figure 1C–1E). Slight differences in the severity of overall growth defects were present in individual transgenic lines, with lines 11 and 14 representing relatively weak and strong alleles, respectively. PCR-based genotyping confirmed that these small seedlings represent homozygous *cdka;1* mutants in segregating T_2 populations (Supplemental Figure 1H and 1I). Similar to wild-type plants, all pollen grains of T_3 *cdka;1*$^{+/-}$ *LAT52pro:CDKA;1 LAT52pro:CDKA;1* plants contained three nuclei. These lines also produced viable seeds (Supplemental Figure 1B and 1G).

In the strong *cdka;1* mutant line 14, only a few pavement cells were present in the cotyledon epidermis (Figure 1A and 1B). The relatively weak *cdka;1* line 11, which has slightly larger seedlings, did harbor some asymmetric divisions and stomata in cotyledons (Figure 1C and 1D). However, all *cdka;1* mutant lines showed significant reductions in stomatal density and index. These lines completely lacked stomata in hypocotyls, indicating that this organ might be more sensitive to the loss of CDKA;1 activity (Table 1). Quantitative (q) RT–PCR analysis showed a significant decrease in *CDKA;1* transcription in both homozygous *cdka;1* mutant lines (Supplemental Figure 1J). The *cdka;1* mutant recovered using a *LAT52pro:CDKA;1* construct, displays defects in root development and SAM maintenance (Supplemental Figure 2), findings consistent with previous observations (Gaamouche et al., 2010; Nowack et al., 2012). The strong *ckda;1* mutant line 14 was used in the remaining experiments.

CDKA;1 Is Required for the Function of SPCH in Entering the Stomatal Lineage

TMM encodes a Leucine-Rich Repeat Receptor-Like Protein that regulates stomatal production and patterning (Nadeau and Sack, 2002b). *TMMpro:TMM-GFP* expression is specific to the stomatal lineage and is present around the time of asymmetric division. The lack of detectible fluorescence from this marker in developing *cdka;1* cotyledons indicates that the loss of *CDKA;1* function blocks entry into the stomatal cell lineage (Figure 1E and 1F). The expression of *BASLpro:GFP-BASL*, whose subcellular localization denotes the fate and placement of divisions in the stomatal lineage (Dong et al., 2009), is also absent from the *cdka;1* epidermis (Figure 1G and 1H). Thus *CDKA;1* is essential for conferring the fate of the MMC, a key

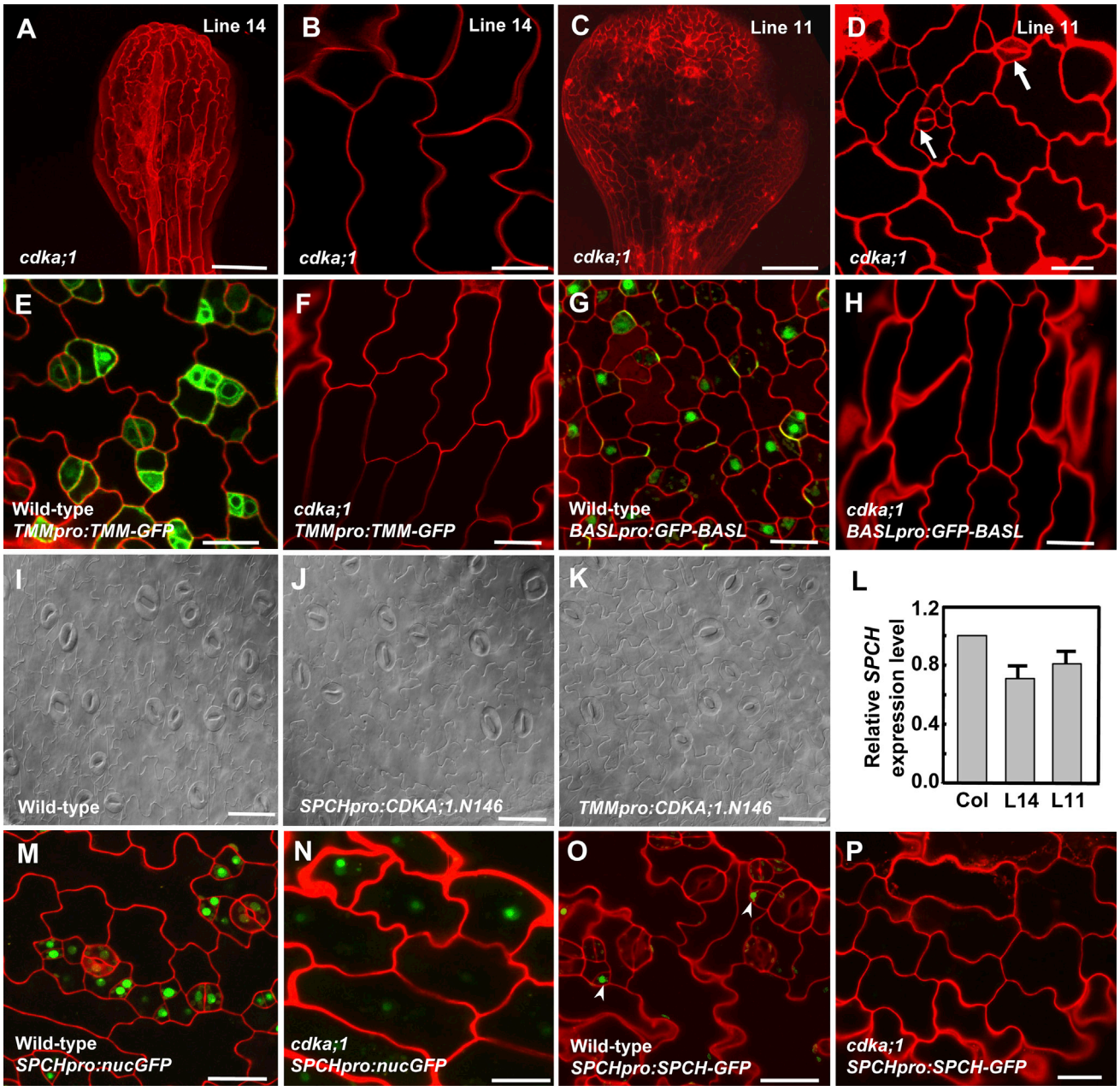

Figure 1. SPCH Function Depends on the Expression of *CDKA;1*.

(A–D) Cotyledon growth is strongly inhibited in a severe *cdka;1* mutant seedling from line 14 **(A)** and slightly less so in the weak line 11 **(C)**. Stomata are absent from the cotyledon epidermis in line 14 **(B)**. A few stomata can be found in the cotyledon epidermis in the weak transgenic line 11 **(D)**. Arrows indicate stomata.

(E and F) *TMMpro:TMM-GFP* is expressed in stomatal lineage cells in the wild-type **(E)** but not in the *cdka;1* **(F)** cotyledon epidermis.

(G and H) *BASLpro:GFP-BASL* expression in cotyledons is present in the wild-type **(G)** but not in the *cdka;1* **(H)** cotyledon epidermis.

(I–K) Differential Interference Contrast (DIC) images of the cotyledon epidermis in wild-type and transgenic plants harboring the dominant-negative *CDKA;1.N146* construct driven by either the *SPCH* or *TMM* promoters. Compared with the wild-type **(I)**, *SPCHpro:CDKA;1.N146* **(J)** and *TMMpro:CDKA;1.N146* **(K)** display reduced stomatal production.

(L) Real-time PCR shows a slight reduction (about a 20%–30%) in *SPCH* transcription levels in *cdka;1* transgenic lines 14 and 11.

(M) A wild-type cotyledon showing fluorescence from a *SPCHpro:nucGFP* transcriptional fusion construct in the stomatal lineage as well as in adjacent young cells.

(N) In *cdka;1*, *SPCHpro:nucGFP* fluorescence persists in most epidermal cells.

(O) Fluorescence from a *SPCHpro:SPCH-GFP* translational fusion construct in the wild-type epidermis is present mostly in meristemoids (arrowheads).

(P) *cdka;1* epidermis showing the absence of *SPCHpro:SPCH-GFP* fluorescence.

Scale bars represent 100 μm in **A** and **C**; 20 μm in **B**, **D**, **E–H**, **I–K**, and **M–P**.

Genotype	Cotyledon stomatal density (number/mm^2)	Cotyledon stomatal index (%)	Hypocotyl stomatal number (number/hypocotyl)
Wild-type	167 ± 4	34 ± 1	18 ± 2
cdka;1 line 11	110 ± 8[a]	20 ± 1[a]	0[a]
cdka;1 line 14	0[a]	0[a]	0[a]
SPCHpro:CDKA;1.N146	111 ± 9[a]	27 ± 0.8[a]	13 ± 1[a]
TMMpro:CDKA;1.N146	104 ± 13[a]	26 ± 0.7[a]	11 ± 2[a]

Table 1. Quantification of Stomatal Formation in *cdka;1* Mutants and *CDKA;1.N146* Transgenic Lines.
Values are average ± SD.
[a]Significant differences relative to wild-type plants after Student *t*-test ($P < 0.05$, $n = 400–1000$).

stomatal early precursor cell, whose asymmetric division produced the meristemoids.

A requirement of *CDKA;1* for stomatal lineage fate is supported by results from the targeted expression of a dominant-negative *CDKA;1.N146* construct (Hemerly et al., 1995, 2000; Joubès et al., 2004; Gaamouche et al., 2010) driven by either the *SPCH* or the *TMM* promoter (Nadeau and Sack, 2002b; MacAlister et al., 2007). Transformation with *SPCHpro:CDKA;1.N146* or *TMMpro:CDKA;1.N146* into wild-type plants significantly reduced stomatal density and index, as well the total number of stomata in hypocotyls, indicating that CDKA;1.N146 competes with endogenous CDKs in stomatal lineage initiation (Figure 1I–1K and Table 1). Thus, the loss of function of *CDKA;1* leads to defects in stomatal production that resembles those in *spch* mutants, i.e. by blocking cell fate and entry divisions in the lineage.

Transformation with *SPCHpro:CDKA;1* failed to complement stomatal defects in cotyledons and hypocotyls of *spch-4* null mutants, consistent with *CDKA;1* not acting downstream of *SPCH* (Supplemental Figure 3A–3D). Real-time PCR analysis shows that *SPCH* transcript levels are lower (about 20%–30% reduction) in *cdka;1* mutants compared with the wild-type (Figure 1L). In the wild-type epidermis, fluorescence from a *SPCHpro:nucGFP* is present throughout almost all cells in the stomatal lineage as well as in adjacent cells. Expression of this transcriptional reporter *SPCHpro:nucGFP* persisted in most epidermal cells in *cdka;1* mutants (Figure 1M and 1N). By contrast, expression from the *SPCHpro:SPCH-GFP* translational fusion in the wild-type epidermis is more restricted to meristemoids. However, *SPCHpro:SPCH-GFP* expression is completely absent from the *cdka;1* mutant epidermis (Figure 1O and 1P). Collectively, these data indicate the existence of post-translational regulation of SPCH by CDKA;1 during stomatal initiation.

The Stability of SPCH Requires CDKA;1 *In Vivo*

Treatment with the BR promotes stomatal production by enhancing the stability of SPCH (Gudesblat et al., 2012). We found that the application of 1 μM epibrassinolide (eBL) not only promotes cell elongation but also significantly increases the total number of stomata in wild-type hypocotyls. However, eBL failed to induce the formation of stomata in *cdka;1* hypocotyls (Supplemental Figure 3E–3H). Treatment with BR synthesis inhibitor brassinazole (BRZ) reduced the number of stomata that form in hypocotyls (Gudesblat et al., 2012). *SPCHpro:nucGFP* was widely expressed in both protruding and non-protruding (stomata-forming) epidermal cells. BRZ treatment did not affect the expression pattern of *SPCHpro:nucGFP* in the hypocotyl epidermis (Supplemental Figure 3I and 3J). By contrast, *SPCHpro:SPCH-GFP* expression was mostly found in dividing cells in non-protruding cell files. BRZ treatment blocked asymmetric divisions from non-protruding cell files and reduced the number of cells expressing *SPCHpro:SPCH-GFP* (Supplemental Figure 3K and 3L). These results are consistent with the previous findings that SPCH-GFP protein levels were reduced in BRZ-treated *SPCHpro:SPCH-GFP* plants (Gudesblat et al., 2012).

The absence of SPCH-GFP fluorescence in *cdka;1 SPCHpro:SPCH-GFP* hypocotyls either after either eBL or BRZ treatment, might result from the instability of SPCH-GFP proteins (Supplemental Figure 3M–3O). Using anti-GFP antibodies, we detected SPCH-GFP signal from wild-type but not *cdka;1* mutant plants after BR treatment (Figure 2A).Thus, stomatal production likely requires the CDKA;1-dependent stabilization of SPCH proteins. In addition, yeast two-hybrid assays indicate that SPCH and the dominant-negative form CDKA;1.N146 directly interact (Figure 2B). However, wild-type CDKA;1 does not appear to interact with SPCH, because either this interaction is transient or the complex is not sufficiently stabilized. Results from *in vivo* bimolecular fluorescence complementation (BiFC) assays further support a direct interaction between CDKA;1.N146 and SPCH (Figure 2C).

SPCH has been shown to function as a dimer with ICE1/SCRM or SCRM2 during stomatal initiation (Kanaoka et al., 2008). The *ice1-2 scrm2-1* double mutant lacks stomata so that the epidermis only contains pavement cells, a phenotype comparable with that of *spch* or *cdka;1* mutants (Supplemental Figure 4A and 4B). *ICE1pro:ICE1-GFP* is normally expressed in stomatal lineage cells, but its fluorescence was not detected in the *cdka;1* epidermis, indicating that CDKA;1 is also likely required for ICE1/SCRM expression (Supplemental Figure 4C and 4D).

CDKA;1 Phosphorylates SPCH *In Vitro*

To test whether SPCH might be a CDKA;1 phosphorylation substrate, we analyzed the amino acid sequence of the SPCH protein and found it harbors 13 possible CDK phosphorylation target sites (S/TP) (Supplemental Figure 5). Three are high-stringency consensus sites for CDK phosphorylation (S/T-P-X-K/R) (Beaudette et al., 1993), i.e. SPKR(65–68), SPRK(186–189), and SPYR(219–222). Residues in SPKR(65–68) are located outside

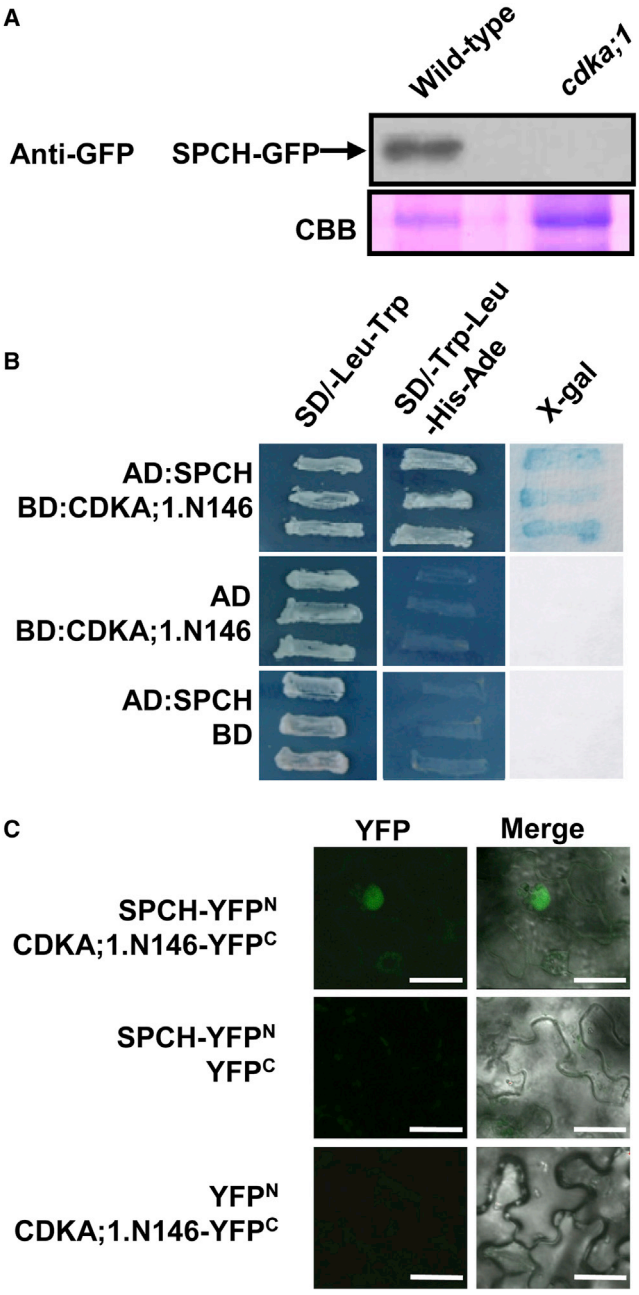

Figure 2. CDKA;1 Directly Interacts with SPCH.
(A) SPCH-GFP protein was not detected in Western blots from *cdka;1* seedlings harboring *SPCHpro:SPCH-GFP* that were grown on BR-supplemented medium (1 μM eBL). The bottom box shows the loading controls after Coomassie brilliant blue (CBB) gel staining.
(B and C) The CDKA;1.N146 protein binds SPCH in yeast two-hybrid **(B)** and BiFC assays **(C)**. Scale bars represent 20 μm.

the MPKTD but overlap with a BIN2-targeted residue Serine 65. Both SPRK(186–189) and SPYR(219–222) are located within the MPKTD (Figure 3A).

We then performed *in vitro* kinase assays using active CDK–Cyclin protein complexes expressed and purified from *Escherichia coli* (Harashima and Schnittger, 2012). The combination of CDKA;1, CYCD3;1, and CDKF;1 (a Cak1 homolog in *Arabidopsis* that is required for CDK–Cyclin complex activity) showed high activity against the histone H1, a control generic kinase substrate (Dissmeyer and Schnittger, 2011). The CDKA;1 showed a kinase activity against SPCH. The MUTE and FAMA bHLH transcription factors, which are closely related to SPCH but lack the typical CDK phosphorylation consensus sequence S/T-P-X-K/R, were not phosphorylated by CDKA;1 complexes (Figure 3B). By contrast, the phosphorylation levels of a mutated SPCH$^{SPKR(65-68)A/\Delta186-222}$ protein, in which the three putative CDK target sites were substituted with non-phosphorylatable alanines or deleted, was greatly decreased (Figure 3C). In addition, we found that a single residue substitution of Serine 186 (SPCH^{S186A}) caused a 40%–50% reduction in phosphorylation, indicating that Serine 186 might play a crucial role in SPCH phosphorylation by CDKA;1 (Figure 3D). The remaining *in vitro* phosphorylation from SPCH^{S186A} might reflect the contribution of other CDK targeted S/T-P residues.

Phosphorylation at Serine 186 Is Required for the *In Planta* Function of SPCH

To identify the phosphorylation sites of SPCH targeted by CDKA;1, multiple SPCH variants were generated in which target residues were substituted or deleted (Figure 4 and Supplemental Table 1). First, *SPCH* variants driven by the native promoter were introduced into *spch-4* null mutants to evaluate their ability to rescue stomatal production. Transgenic lines with comparable *SPCH* transcript levels were used for rescue assays (Supplemental Figure 6A). SPCH phosphorylation-deficient mutants, SPCH$^{SPKR(65-68)A}$, in which four residues SPKR were substituted with alanines, or SPCH$^{SPYR(219-222)A}$, in which the SPYR residues were substituted with alanines, still could restore stomatal production in the *spch-4* null mutant allele (Figure 4A and 4B). By contrast, SPCH$^{SPRK(186-189)A}$ variant, in which the SPRK residues were substituted with alanines, failed to rescue *spch-4* stomatal defects, indicating that phosphorylation of SPRK186 residues is required for SPCH function in producing stomata (Figure 4C). The transformation *SPCH*$^{SPKR(65-68)A/SPRK(186-189)A}$, a construct carrying mutations in SPRK with the addition of SPKR, yielded a phenotype similar to that of *SPCHpro:SPCH*$^{SPRK(186-189)A}$ (Figure 4D). The *SPCHpro:SPCH*$^{SPKR(65-68)A/\Delta186-222}$ variant in which all three predicted CDK target sites were eliminated consistently failed to complement the *spch-4* mutant as well, indicating that SPRK is essential for SPCH function (Figure 4E). We also generated an SPCH^{S186A} variant in which only the Serine 186 underwent alanine substitution. Like *SPCH*$^{SPRK(186-189)A}$, the expression of *SPCH*^{S186A} also failed to rescue *spch-4* stomatal defects (Figure 4F).

A mild gain of function of *SPCH* gene, i.e. the expression of *SPCHpro:SPCH-GFP* in the wild-type epidermis, induced extra asymmetric divisions and excess stomata (Figure 1G) (MacAlister et al., 2007). However, the expression of either *SPCH*$^{SPRK(186-189)A}$ or *SPCHpro:SPCH*$^{SPKR(65-68)A/\Delta186-222}$ driven by the *SPCH* promoter in the wild-type epidermis failed to induce the formation of extra stomata, indicating that SPCH phosphorylation at SPRK186 is essential for the SPCH gain-of-function phenotype (Figure 4G and 4H; Supplemental Figure 7).

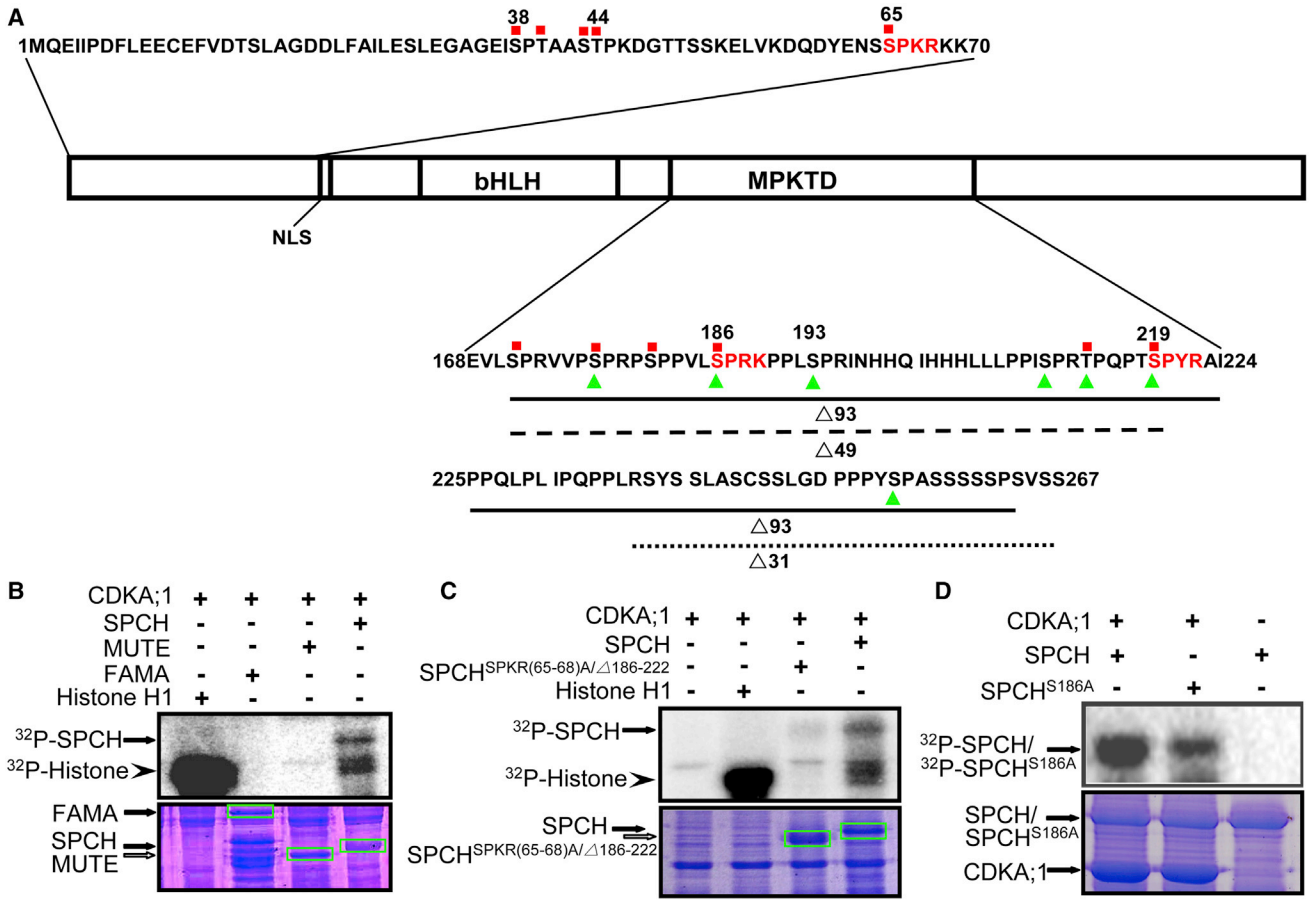

Figure 3. SPCH Is Phosphorylated by the CDKA;1 Complex.

(A) Schematic diagram of phosphorylation sites in the SPCH protein. Red letters indicate three predicted phosphorylation sites by CDKA;1 in the SPCH protein. Red squares mark BIN2 phosphorylation target sites. Green triangles indicate MPK phosphorylation target sites. Deletions are shown as solid underline for SPCH Δ93, long-dashed underline for SPCH Δ49, and a short-dashed underline for SPCH Δ31 (according to Lampard et al., 2008).

(B) Autoradiographs show that SPCH was phosphorylated by active CDKA;1 complexes (CDKA;1-CYCD3;1-CDKF;1). By contrast, the MUTE and FAMA proteins were not phosphorylated by CDKA;1.

(C and D) The extent of phosphorylation of the mutated SPCH proteins, $SPCH^{SPKR(65-68)A/\Delta 186-222}$ **(C)** and $SPCH^{S186A}$ **(D)**, was obviously reduced. The bottom boxes in **(B–D)** show the loading controls after Coomassie brilliant blue gel staining.

Phosphorylation at Serine 186 Promotes Stomatal Production

Multiple residues within the MPKTD are important for the function of SPCH. The partial deletion or substitution of these residues leads to excessive numbers of asymmetric cell divisions (Lampard et al., 2008). For example, the expression of the *SPCH Δ93* construct, in which the entire MPKTD was deleted, in wild-type plants resulted in the formation of many stomata in direct contact (Figure 5A). Expression of $35Spro:SPCH^{S/T38\text{-}44A}$, in which the BIN2-targeted S/T residues between 38S and 44T (Gudesblat et al., 2012, indicated in Figure 3A) were substituted with alanines, induced extra divisions outside the stomatal cell lineage (Figure 5B). These additional divisions increased total epidermal cell number and lowered the stomatal index. We then generated an SPCH variant $SPCH^{S/T38\text{-}44/\Delta 93}$, in which an MPKTD deletion was combined with the disruption of key BIN2 target sites (38S-44T). Large stomatal clusters were present in the $SPCH^{S/T38\text{-}44/\Delta 93}$ epidermis (Figure 5C).

Although the phosphorylation of Serine 186 has been identified by mass spectrometry, the functional specificity of this residue has yet to be reported (Lampard et al., 2008; Gudesblat et al., 2012). We generated a phosphorylation-mimic variant $SPCH^{S186D}$, in which Serine 186 was replaced with aspartic acid residue, and transformed it into the wild-type plants. Surprisingly, about 40% of $35Spro:SPCH^{S186D}$ transgenic lines displayed stomatal clusters and increased stomatal density, indicating that phosphorylation at Serine 186 of SPCH promotes stomatal production (Figure 5D and Table 2). To address whether phosphorylation-mimic $SPCH^{S186D}$ can complement stomatal production in *cdka;1*, we crossed a $35Spro:SPCH^{S186D}$ line (Figure 5E and Table 2) that showed normal stomatal production with $cdka;1^{+/-}$ *LAT52pro:CDKA;1* seedlings. Possibly because of the broad functions of CDKA;1 in many aspects of plant development than that of SPCH, we were unable to recover transformants. Since the stomatal production was inhibited by targeted expression of

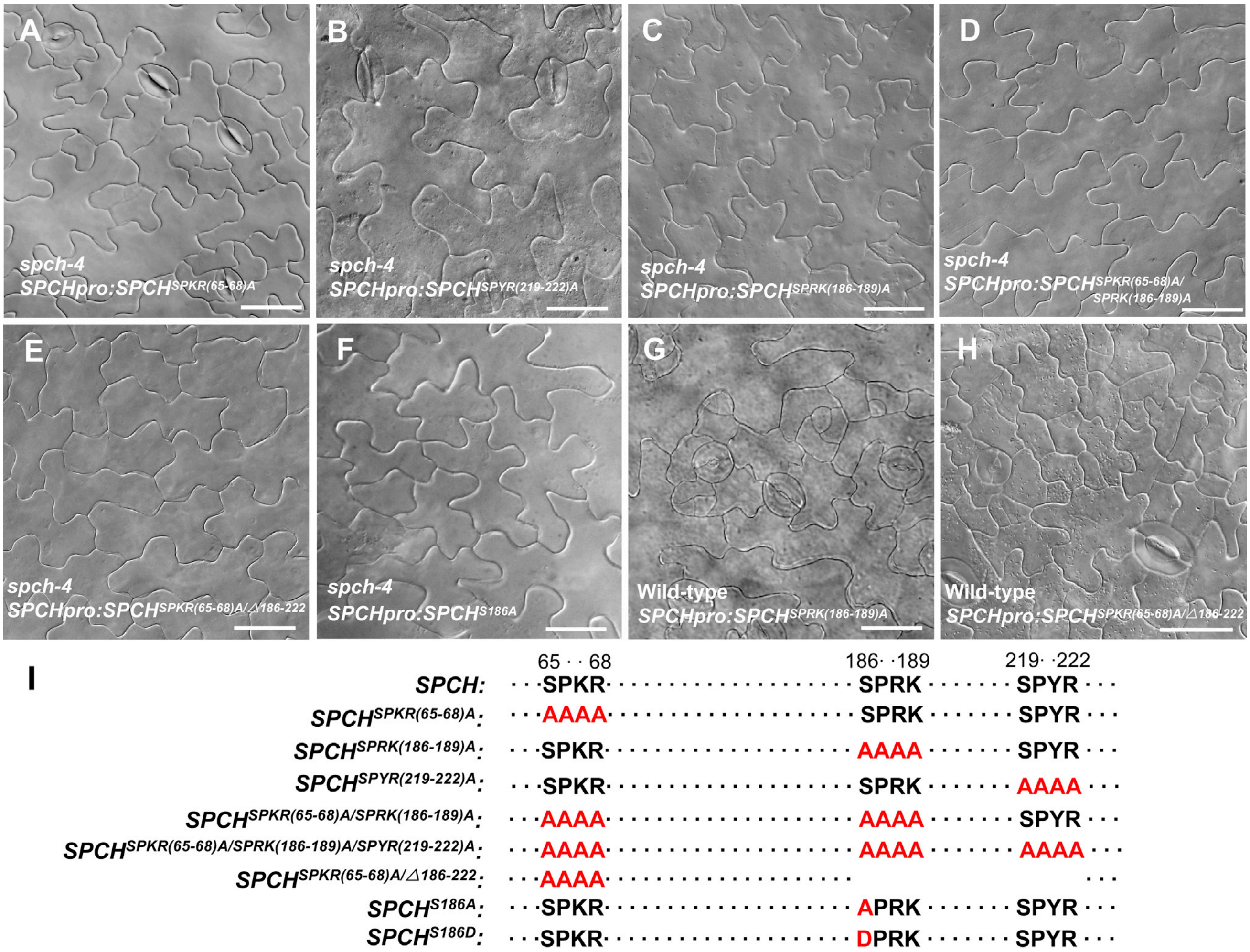

Figure 4. Expression of Different SPCH Variants Induces Distinct Epidermal Phenotypes.

(A–F) DIC images from mature leaves of an *spch-4* mutant transformed with SPCH variants. Stomatal defects in the *spch-4* allele are rescued by *SPCHpro:SPCH*$^{SPKR(65\text{-}68)A}$ **(A)** and the *SPCHpro:SPCH*$^{SPYR(219\text{-}222)A}$ **(B)**, but not by *SPCHpro:SPCH*$^{SPRK(186\text{-}189)A}$ **(C)**, *SPCHpro:SPCH*$^{SPKR(65\text{-}68)A/SPRK(186\text{-}189)A}$ **(D)**, *SPCHpro:SPCH*$^{SPKR(65\text{-}68)A/\Delta 186\text{-}222}$ **(E)**, or *SPCHpro:SPCH*^{S186A} **(F)**.

(G and H) DIC images of the epidermis of mature leaves of wild-type plants transformed with SPCH variants driven by the *SPCH* native promoter. Transformation with *SPCHpro:SPCH*$^{SPRK(186\text{-}189)A}$ **(H)** and *SPCHpro:SPCH*$^{SPKR(65\text{-}68)A/\Delta 186\text{-}222}$ **(I)** induces excess cell divisions but does not induce the formation of extra stomata.

Scale bars represent 20 μm.

(I) Schematic diagram shows the SPCH variants.

SPCHpro:CDKA;1.N146 (Figure 1J), alternatively we crossed *35Spro:SPCH*^{S186D} with an *SPCHpro:CDKA;1.N146* line. The introduction of *SPCH*^{S186D} can fully restore normal stomatal production in *SPCHpro:CDKA;1.N146* (Figure 5F and Table 2), demonstrating the physiological significance of CDKA;1 phosphorylation at Serine 186 of SPCH in promoting stomatal initiation.

Overexpression of Phosphorylation-Deficient *SPCH* Induced Excess Physically Asymmetric Divisions but Not Stomata

Constitutive expression of *SPCH* driven by the 35S promoter in the wild-type plants induced extra cell divisions, such as additional symmetric divisions in pavement cells, which could be recognized by the straight wall within the lobbed pavement cells (Figure 6A) (MacAlister et al., 2007; Lampard et al., 2008). Since *spch* mutants block entry into stomatal lineage, we further characterized the *in planta* functions of CDK phosphorylation on SPCH by transforming the CDK phosphorylation-deficient version of *SPCH* into wild-type plants that was driven by the 35S promoter. However, about 40%–50% of the transgenic lines exhibited an *spch* mutant phenotype that might arise from the silencing of SPCH activity (MacAlister et al., 2007). Transformed lines were then selected for phenotypic analysis based upon transcript levels assessed using real-time PCR (Supplemental Figure 6B–6E).

As with *35Spro:SPCH*, the *35Spro:SPCH*$^{SPKR(65\text{-}68)A}$ and *35Spro:SPCH*$^{SPYR(219\text{-}222)A}$ lines harbored extra symmetric divisions in pavement cells, resulting in a decrease in the stomatal index (Figure 6B and 6C; Supplemental Table 2). Strikingly, in

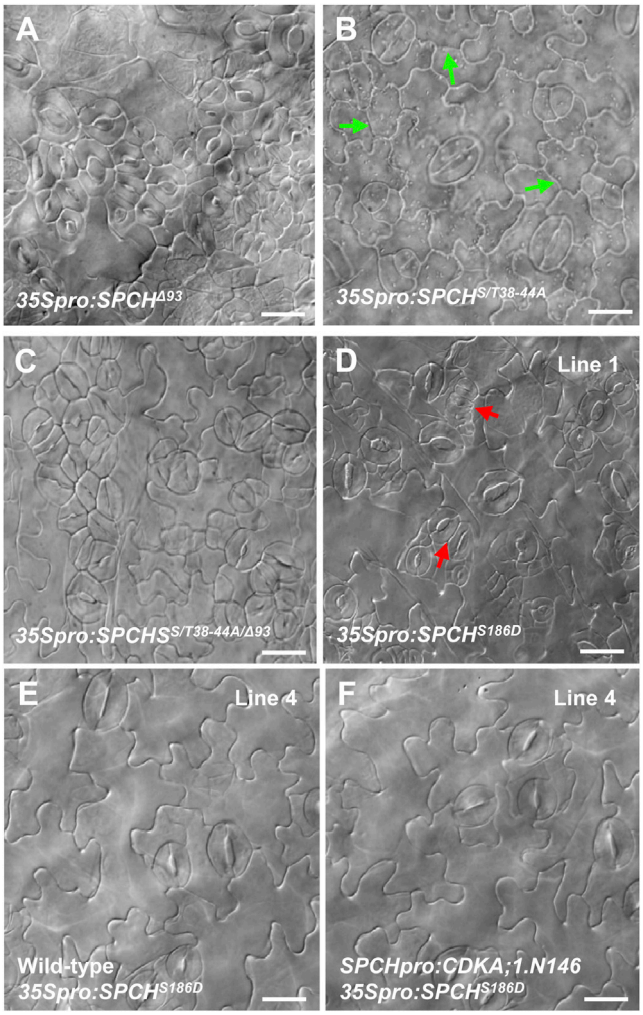

Figure 5. Phosphorylation at Serine 186 Promotes Stomatal Production.
(A) Extensive clusters arise in *35pro:SPCH*$^{\Delta 93}$.
(B) Expression of *35Spro:SPCH*$^{S/T38\text{-}44A}$ induces ectopic symmetric divisions in pavement cells, indicated by green arrows.
(C) Stomatal clusters in *35pro:SPCH*$^{S/T38\text{-}44A/\Delta 93}$.
(D) Stomatal clusters in *35Spro:SPCH*^{S186D} line 1, indicated by red arrows.
(E) No stomatal clusters found in *35Spro:SPCH*^{S186D} line 4.
(F) Expression of *35Spro:SPCH*^{S186D} rescued the stomatal phenotypes in *SPCHpro:CDKA;1.N146*. See the quantitative analysis in Table 2.
Scale bars represent 20 μm.

addition to the symmetric divisions in pavement cells, *35Spro:SPCH*$^{SPRK(186\text{-}189)A}$ expression induced the formation of an excessive number of small cells that resembled stomatal precursors (Figure 6D). Consistent with the phenotypes of *SPCH*$^{SPRK(186\text{-}189)A}$, the constitutive expression of *35Spro:SPCH*^{S186A} also induced the formation of ectopic divisions in epidermis (Figure 6E).

However, most of these precursor-like cells failed to develop into stomata, resulting in a significant decrease in the stomatal index in *SPCH* $^{SPRK(186\text{-}189)A}$ transgenic lines (Supplemental Table 2). We then evaluated the expression of the stomatal lineage marker *TMMpro:TMM-GFP* in a *SPCH*$^{SPRK(186\text{-}189)A}$ epidermis. Except for a low fraction of cells, no GFP signal was detected

Genotype	Stomatal density (number/mm^2)
35Spro:SPCH^{S186D} line 1	297 ± 37 Aa
35Spro:SPCH^{S186D} line 4	159 ± 4.3 Bb
Wild-type	163 ± 5.5 Bb
SPCHpro:CDKA;1.N146	124 ± 8.2 Bc
SPCHpro:CDKA;1.N146 *35Spro:SPCH*^{S186D} line 4	151 ± 4.5 Bb

Table 2. Quantification of Stomata Production Promoted by Expression of the Phosphorylation-Mimic Version *SPCH*^{S186D}.
Data were analyzed using ANOVA. The different uppercase and lowercase letters indicate significant differences at 1% and 5% levels, respectively (n = 800–1200).

in most of these small epidermal cells produced by excess asymmetric division (Figure 6F). Moreover, the expression of *MUTEpro:MUTE-GFP*, which marks stem cells at the meristemoid to GMC transition, was often absent in these precursor-like cells (Figure 6G).

Expression of *35Spro:SPCH*$^{SPKR(65\text{-}68)A/SPRK(186\text{-}189)A}$ induced more asymmetric divisions in the epidermis compared with the *35Spro:SPCH*$^{SPRK(186\text{-}189)A}$ construct, resulting in a lowered stomatal index (Figure 6H and Supplemental Table 2). The number of non-stomatal cells increased in *35Spro:SPCH*$^{SPKR(65\text{-}68)A/SPRK(186\text{-}189)A/SPYR(219\text{-}222)A}$ background as well as in *35Spro:SPCH*$^{SPKR(65\text{-}68)A/\Delta 186\text{-}222}$ transgenic lines, resulting in a further decrease in the stomatal index (Figure 6I and 6J; Supplemental Table 2). Although expression from *TMMpro:TMM-GFP* and *MUTEpro:MUTE-GFP* expression was occasionally found in some epidermal cells, most precursor-like cells failed to express these GFP constructs (Figure 6K and 6L). These findings indicate that the overexpression of the CDK phosphor-deficient version of *SPCH* can trigger excess physically asymmetric divisions in the epidermis but cannot confer a stomatal fate.

DISCUSSION

Transformation with a *LAT52pro:CDKA;1* construct fully prevents the abortion of homozygous *cdka;1* seeds. This enables the characterization of many CDKA;1 functions such as exist in stomatal development. Our results are consistent with a previous report showing phenotypic abnormalities in homozygous *cdka;1* mutants (Nowack et al., 2012). The expression of dominant-negative *CDKA;1.N146* construct might reduce overall CDK activity by competing with the endogenous CDKs in binding cyclin subunits (Gaamouche et al., 2010). Besides blocking GMC symmetric divisions, the loss-of-function *cdkb1;1 cdkb1;2* double mutant as well as the *35Spro:CDKB1;1.N161* line display reduced stomatal density, indicating that *CDKB1*s might also regulate stomatal initiation (Boudolf et al., 2004; Xie et al., 2010). However, the expression of *CDKB1;1* under the control of the *CDKA;1* native promoter in a *cdka;1* mutant background led to the formation of only a limited number of stomata (Weimer et al., 2012). Thus, stomatal initiation is primarily regulated by CDKA;1, although it cannot be ruled out that other CDKs, such as CDKB1s and CDKB2s, contribute to these processes as well (Figure 7).

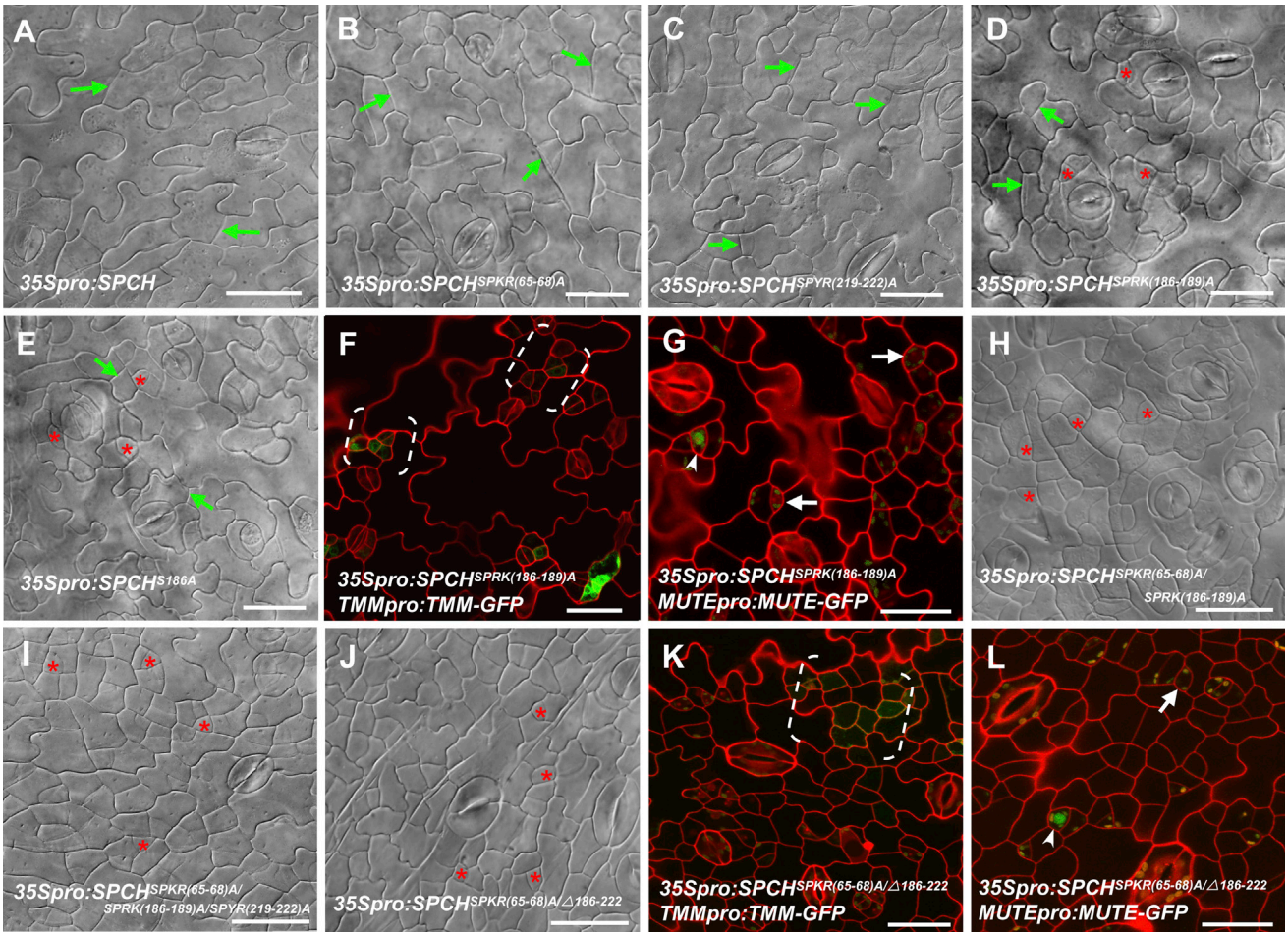

Figure 6. Expression of Different SPCH Variants Induces Distinct Epidermal Phenotypes.

(A–C) DIC images from mature leaves of wild-type plants transformed with *35Spro:SPCH* **(A)**, *35Spro:SPCH*$^{SPKR(65-68)A}$ **(B)**, and *35Spro:SPCH*$^{SPYR(219-222)A}$ **(C)**. Green arrows indicate ectopic symmetric divisions in pavement cells.

(D and E) Besides symmetric divisions in pavement cells, expression of *35Spro:SPCH*$^{SPRK(186-189)A}$ **(D)** and *35Spro:SPCH*^{S186A} **(E)** also induces excess physically asymmetric divisions. Red stars mark precursor-like cells.

(F and G) Most precursor-like cells in a *35Spro:SPCH*^{S186A} epidermis fail to express the stomatal lineage marker *TMMpro:TMM-GFP* **(F)** as well as *MUTEpro:MUTE-GFP* **(G)**.

(H–J) DIC images from mature leaves of *35Spro:SPCH*$^{SPKR(65-68)A/SPRK(186-189)A}$ **(H)**, *35Spro:SPCH*$^{SPKR(65-68)A/SPRK(186-189)A/SPYR(219-222)A}$ **(I)**, and *35Spro:SPCH*$^{SPKR(65-68)A/\Delta 186-222}$ **(J)**. Red stars mark precursor-like cells.

(K and L) Excessive divisions produce extra small cells in the *35Spro:SPCH*$^{SPKR(65-68)A/\Delta 186-222}$ epidermis. However, most of the precursor-like cells fail to express *TMMpro:TMM-GFP* **(K)** and *MUTEpro:MUTE-GFP* **(L)**.

Brackets in **(F)** and **(K)** indicate patchy expression of *TMMpro:TMM-GFP*. Arrowheads in **(G)** and **(L)** indicate occasional *MUTEpro:MUTE-GFP* fluorescence in GMCs. Arrows point to GFP-negative precursor-like cells.

Scale bars represent 20 μm.

CDKA;1 has been previously reported to influence *Arabidopsis* stomatal development in both formative asymmetric divisions and terminal symmetric divisions (Weimer et al., 2012; Yang et al., 2014). SPCH is proposed to be transcriptionally regulated by CDKA;1 via the regulation of RBR activity (Weimer et al., 2012). Recent studies also indicate that FAMA or FLP interacts with RBR to maintain GC fate by a possible suppression of SPCH in GCs (Lee et al., 2014). However, we found *SPCH* transcription levels to be about 20%–30% reduced in *cdka;1* mutants compared with the wild-type. In contrast to the persistent expression of the *SPCHpro:nucGFP* transcriptional reporter, the absence of *SPCHpro:SPCH-GFP* expression and the inability to detect any SPCH-GFP protein in *cdka;1* indicate that CDK activity is also required for SPCH protein stabilization (Figure 7).

SPCH has already been shown to be a substrate of the MPKs and the BIN2 kinases (Lampard et al., 2008; Gudesblat et al., 2012). Unlike MUTE and FAMA, SPCH harbors a unique MAPK target domain that contains five high-stringency MPK phosphorylation sites. Expression of SPCH variants harboring the deletion of the entire MPKTD (SPCH Δ93) or substitutions of all five target sites with alanines (SPCH S1–5) leads to excessive stomatal formation, and indicates that all five MPK phosphorylation sites are important for SPCH function since partial deletion or substitution of MPK target sites failed to induce stomatal clusters (Lampard

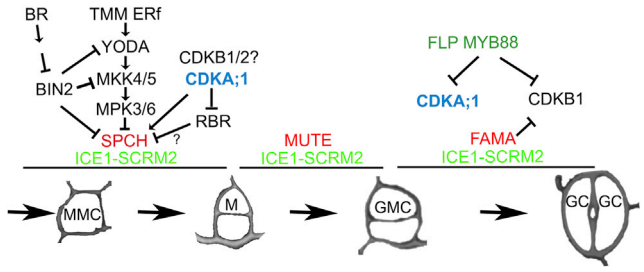

Figure 7. Schematic Diagram of Stomatal Development and Its Regulatory Pathway.

The bHLH transcriptional factor *SPEECHLESS* (*SPCH*) controls entry into the stomatal cell lineage by first forming a Meristemoid Mother Cell (MMC). The MMC divides asymmetrically, yielding a Meristemoid (M) and a larger sister cell. SPCH is a phosphorylation target of a signal transduction cascade that includes MAPKKK (YODA), MKK4/5, and MPK3/6. Brassinosteroid (BR) regulates stomatal initiation via BIN2 kinase, which directly or indirectly (via MAPK cascade) phosphorylates SPCH. CDKA;1 promotes stomatal initiation by enhancing SPCH activity. Levels of *SPCH* transcription are likely regulated by RBR, which is targeted by CDKA;1. MUTE is a key bHLH transcription factor required for the fate transition from M to Guard Mother Cell (GMC). FAMA, which is also a bHLH transcription factor, as well as the R2R3 MYB transcription factors FOUR LIPS (FLP) and MYB88, restrict GMC divisions to one, thus ensuring that stomata consist of only two GCs. Loss of CDKA;1 or CDKB1 activity blocks GMC division, resulting in single guard cells. *CDKB1* and *CDKA;1* transcription is negatively regulated by FLP/MYB88 and FAMA. The heterodimerization of ICE1 and SCRM2 with SPCH, MUTE, and FAMA is required respectively for stomatal initiation, the meristemoid to GMC transition, and GC differentiation.

et al., 2008). By contrast, we show here that a phosphorylation-mimic variant carrying a single residue substitution of Serine 186 ($SPCH^{S186D}$) leads to the formation of excessive number of stomata in contact, a phenotype that resembles that in plants expressing MPK phosphorylation-deficient variants, such as SPCH Δ93 or SPCH S1–5 (Lampard et al., 2008). In addition, the phosphorylation-mimic $SPCH^{S186D}$ can fully rescue defective stomatal production in *SPCHpro:CDKA;1.N146* transgenic lines, demonstrating that CDK phosphorylation of SPCH at Serine 186 promotes SPCH function in stomatal initiation.

Interestingly, the Serine 193 residue in SPCH, which is a MPK phosphorylation target located close to the Serine 186 residue, behaves differently from other MPK target residues with respect to SPCH function (Lampard et al., 2008). Non-phosphorylatable SPCH at both Serine 193 and Serine 186 failed to rescue stomatal production in *spch* null mutants. This suggests that the phosphorylation of Serine 186 and Serine 193 is positively required for SPCH function in promoting the entry of stomatal lineage, although the relationship between Serine 193 and Serine 186 remain to be determined. The Serine 193 residue has been implicated in the initial phosphorylation of SPCH that leads to SPCH protein activation, either by altering the binding affinity of SPCH for target DNA or by changing the ability of SPCH to interact with partner proteins (Lampard, 2009). This would be similar to the phosphorylation of Replication Protein A (RPA) that is a heterotrimeric protein required for DNA replication, repair, and recombination, and the response to DNA damage. The phosphorylation of the 32-kDa subunit of RPA by multiple kinases affects the binding activity of RPA with dsDNA. The initial phosphorylation by Cdk1/2 on the Serine 23 and Serine 29 residues is required for RPA binding activity to DNA and additional phosphorylation by other kinases, i.e. ATM and DNA-dependent protein kinase (Oakley and Patrick, 2012). We hypothesize that CDK phosphorylation at Serine 186 residue of SPCH might impact additional phosphorylations of SPCH, e.g. either by the same phosphorylation residues with MPKs/BIN2 or by altering the SPCH protein conformation required for consequent phosphorylation by MPKs/BIN2. Mass spectrometry analyses also showed that BR treatment caused the dephosphorylation of Serine 186 (Gudesblat et al., 2012), indicating that the phosphorylation status of Serine 186 might also be involved in the MPK/BIN2-mediated SPCH phosphorylation downstream of BR signals. However, a remaining major challenge is to define how SPCH proteins are selectively or co-ordinately phosphorylated by multiple kinases in different cell types, organs, and developmental stages in response to intrinsic and extrinsic signals (Wengier and Bergmann, 2012; Le et al., 2014; Wang et al., 2014).

Constitutive expression of *SPCH* driven by the 35S promoter induced extra symmetric divisions in pavement cells, suggesting a role of SPCH in promoting cell proliferation. Overexpression of phosphorylation-deficient $SPCH^{SPRK(186\text{-}189)A}$ alone stimulated physically asymmetric divisions. Overexpression of $SPCH^{SPKR(65\text{-}68)A/SPRK(186\text{-}189)A/SPYR(219\text{-}222)A}$ or $SPCH^{SPKR(65\text{-}68)A/\Delta 186\text{-}222}$ induced stronger effects on stimulating divisions, thus mimicking the epidermal phenotype of *SPCH Δ49* overexpressing plants (indicated in Figure 3A; Lampard et al., 2008). The absence of the expression of stomatal lineage markers in these small cells produced by extra divisions is consistent with the observation that the physical asymmetry of excessive divisions can be uncoupled from asymmetric cell fate (Qian et al., 2013). By contrast, expression of another MPKTD-deletion SPCH variant, *SPCH Δ31*, which retains Serine 186 (indicated in Figure 3A), allows asymmetric divisions as well as stomatal formation in an *spch* mutant background (Lampard et al., 2008).

Since *SPCH* is initially expressed in all protodermal cells, it has been suggested that ICE1/SCRM and SCRM2 function as partners in specifying the fate of MMCs that are required to initiate formation of stomata (Kanaoka et al., 2008) (Figure 7). Loss-of-function mutations in both *ICE1/SCRM* and *SCRM2* also block entry into the stomatal lineage, resulting in an epidermis consisting of just non-stomatal cells (i.e. pavement cells), a phenotype that resembles that of *spch* or *cdka;1* mutants. The opposite phenotype, an epidermis consisting only of stomata, is present in the gain-of-function *ICE1/SCRM scrm-D* allele. The R236H mutation in *scrm-D* enhances the interaction of SPCH with ICE1/SCRM and stabilizes SPCH activity in all epidermal cells. The expression and activity of SPCH or ICE1/SCRM presumably depends upon each other's expression as well as the formation of their heterodimers (Kanaoka et al., 2008). The absence of *ICE1/SCRM* expression in the *cdka;1* mutant might result from the instability of the SPCH protein. It is also possible that the absence of SPCH phosphorylation in a *cdka;1* mutant disrupts interactions between ICE1/SCRM and SPCH that in turn lead to the loss of *ICE1/SCRM* expression. The formation of excessive numbers of small cells in transgenic lines harboring SPCH variants resembles the phenotype of *scrm-D*/+ heterozygotes

or of *spch*/+ *scrm-D* double mutant. It is thus likely that the phosphorylation of SPCH by CDKA;1 might be also important for the formation of SPCH-ICE1/SCRM heterodimers by maintaining the stability or activity of the SPCH protein, thereby ensuring stomatal cell fate.

METHODS

Plant Materials and Treatment

All genotypes were in a Columbia (Col-0) ecotypic background. Seeds of *cdka;1*$^{+/-}$ (SALK_106809) and *spch-4* (SALK_078595) were obtained from the *Arabidopsis* Biological Resource Center (ABRC); the presence of the mutations was confirmed using PCR. All *Arabidopsis* lines were grown at 22°C in a growth room with a 16 h light/8 h dark regime. For the eBL (Sigma) and BRZ (TCI) treatments, seeds were sown on the surface of medium supplemented with 1 μM eBL or 3 μM BRZ.

Plasmid Construction and Plant Transformation

To obtain a viable *cdka;1* mutant, the *LAT52pro:CDKA;1* construct, containing the full-length cDNA of *CDKA;1* under the control of the pollen-specific *LAT52* promoter (Muschietti et al., 1994), was transformed into *Agrobacterium tumefaciens* strain EHA105, and then introduced into heterozygous *cdka;1*$^{+/-}$ plants using the floral dip method (Clough and Bent, 1998). Transgenic plants were selected on half-strength Murashige and Skoog (MS) medium containing 25 μg/ml hygromycin. The homozygosity of *cdka;1* plants was confirmed by PCR analysis using primers shown in Supplemental Table 3.

Constructs and transgenic lines harboring *SPCHpro:CDKA;1.N146* and *TMMpro:CDKA;1.N146* were verified using PCR. Promoter fragments of *SPCH* and *TMM* genes, as well as full-length cDNA clones of *CDKA;1*, were obtained by PCR amplification. The *CDKA;1.N146* dominant-negative construct was generated by introducing a point mutation followed by PCR amplification. All resulting DNA fragments were cloned into the pMD19-T vector (TaKaRa). Fragments were then sub-cloned into a pCAMBIA1300 vector (CAMBIA) and transformed into wild-type plants.

To obtain the SPCH variants SPCH$^{SPKR(65-68)A}$, SPCH$^{SPRK(186-189)A}$, and SPCH$^{SPYR(219-222)A}$, residues of CDK target sites SPKR(65–68), SPRK(186–189), and SPYR(219–222) were replaced with a tetra-alanine linker region, respectively. To obtain the SPCH^{S186A} variant, only serine residue was replaced with alanine. To obtain the SPCH^{S186D} variant, the Serine 186 residue was replaced with aspartic acid. To obtain the SPCH$^{SPKR(65-68)A/SPRK(186-189)A}$ variant, the residues at each of the SPKR(65–68) and SPRK(186–189) sites were replaced with alanines. The SPCH$^{SPKR(65-68)A/SPRK(186-189)A/SPYR(219-222)A}$ variant was generated by replacing the residues in all three CDK target sites with alanines. To obtain the SPCH$^{SPKR(65-68)A/\Delta 186-222}$ variant, in addition to the replacement of the residues of SPKR(65–68) with alanines, residues located between positions 186 and 222 were deleted. SPCH$^{S/T38-44A}$ and SPCH$^{S/T38-44A/\Delta 93}$ DNA was obtained by PCR using plasmids as described in Gudesblat et al. (2012). The resulting SPCH variants were then sub-cloned into a pCAMBIA1300 vector (CAMBIA) driven either by 35S or the *SPCH* native promoter, and then transformed into the wild-type plants or plants harboring the *spch-4* mutation.

Rescue Assays

To assay the ability of *SPCH* variants to rescue the *spch* null mutant phenotype, *SPCH* variants were transformed into *spch-4* heterozygous plants driven by the native *SPCH* promoter. Transgenic plants were screened on media containing 25 μg/ml hygromycin. The T1 transgenic plants were identified by PCR to confirm the homozygosity of the *spch-4* allele as well as the presence of the transgenic insertion. The wild-type and *spch* phenotypes were scored in T2 segregating populations. The significance of phenotypic rescue was evaluated using a chi-square test. A value of 0.25 was used as a cut-off for failure to rescue stomatal production in *spch-4*. Rescue was scored if no T2 seedlings exhibited a *spch*-4 mutant phenotype. Real-time PCR analysis was performed to monitor transcript levels for each line.

Western Blotting

Proteins were extracted from 2 g of 3-day-old wild-type or *cdka;1* seedlings harboring *SPCHpro:SPCH-GFP* that were grown on the surface of medium supplemented with 1 μM eBL. Extraction buffer contained 50 mM Tris–HCl, 150 mM NaCl, 1% NP-40 (pH 7.5), and a protease inhibitor cocktail (Roche Diagnostics). Extracts were centrifuged at 14 000 *g* at 4°C for 40 min. Total protein was then separated using 12% SDS–PAGE and analyzed with an anti-GFP antibody (MBL) at 1:10 000 dilution.

DAPI Staining and Measurement of DNA Content

Visualization of nuclei in pollen grains was as described in Iwakawa et al. (2006).

Microscopy

Two-week-old cotyledons and hypocotyls were cleared as described in Malamy and Benfey (1997). Samples were mounted in 50% glycerol and imaged as above. Cotyledons and hypocotyls were stained with 0.1% (w/v) propidium iodide to visualize cell wall fluorescence. Fusions to GFP and YFP were imaged with an Olympus FV1000-MPE confocal laser scanning microscope.

qRT–PCR

Total RNA from 10-day-old *cdka;1,* wild-type and SPCH variant seedlings were extracted using TRNzol reagent (http://www.tiangen.com). Reverse transcription was performed using a Promega kit (http://www.promega.com). Amplified *ACTIN2* genes were used as an internal control. Real-time quantitative PCR experiments were repeated independently three times. The data were averaged and cDNA was amplified using SYBR Premix ExTaqTM (TaKaRa) with a Corbett Research Rotor-Gene 3000 Thermal Cycler.

Yeast Two-Hybrid Assay

Gal4 system vectors from Clontech (http://www.clontech.com/) were used. The full-length coding sequence of *CDKA;1.N146* was amplified using primers shown in Supplemental Table 3. *CDKA;1.N146* cDNA fragments were cloned into a pGBKT7 vector. Constructs were then co-transformed into an AH109 yeast strain. Co-transformed strains were selected on SD/-Leu-Trp and SD/-Leu-Trp-His-Ade. X-Gal activity was analyzed according to the manufacturer's instructions.

BiFC Assay

Coding sequences of *CDKA;1.N146* and *SPCH* were amplified using the primers shown in Supplemental Table 3. Fragments were then cloned into pSPYNE-35S and pSPYCE-35S vectors to generate the *CDKA;1.N146-YC* (YFP C-terminal) construct and the *SPCH-YN* (YFP N-terminal) constructs, respectively (Walter et al., 2004). *CDKA;1.N146-YC* and *SPCH-YN* were co-transformed into tobacco leaves. Fluorescence was imaged using an Olympus FV1000-MPE confocal laser scanning microscope.

Preparation of CDK–Cyclin Complexes and Kinase Assay

Plasmids of the CDK–Cyclin active complex and proteins were prepared as in Harashima and Schnittger (2012). The full coding sequences of *SPCH*, *SPCH*$^{SPKR(65-68)A/\Delta 186-222}$, *SPCH*^{S186A}, *MUTE*, and *FAMA* were amplified using primers shown in Supplemental Table 3. The *SPCH,* *SPCH*$^{SPKR(65-68)A/\Delta 186-222}$, and *SPCH*^{S186A} sequences were ligated into pET28a. *MUTE* and *FAMA* sequences were ligated into pGEX4T-1. Plasmids were then transformed into the BL21 *E. coli* strain, and cells were grown at 37°C to an OD_{600} equal to 0.6. Cultures were then transferred to 18°C and grown for 30 min. Fusion protein production was induced

by adding 0.4 mM IPTG overnight at 18°C. The wild-type SPCH and mutated SPCH proteins were purified using Ni-NTA agarose (GE). The MUTE and FAMA proteins were purified using GST beads. Kinase assays were carried out as described (Harashima et al., 2007). The kinase assays with 3 μg of recombinant proteins were carried out with 2 μCi [γ-^{32}P]ATP in 20 μl kinase buffer (50 mM Tris–HCl pH 7.5, 10 mM $MgCl_2$, 1 mM EGTA, and 1 mM cold ATP) for 30 min at 30°C. The reaction was stopped by the addition of 4 μl of 5× SDS loading buffer and boiled for 5 min at 100°C. Proteins were separated by 12% SDS–PAGE gels. The autoradiography films can easily be overexposed for histone H1 (Dissmeyer and Schnittger, 2011), but the phosphorylated SPCH could be detected on films after a 5–10 min exposure.

ACCESSION NUMBERS

Sequence data from this article can be found in the *Arabidopsis* Genome Initiative under the following accession numbers: AT3g48750 (*CDKA;1*), AT3g54180 (*CDKB1;1*), AT5g53210 (*SPCH*), AT3g06120 (*MUTE*), AT3g24140 (*FAMA*), AT3g12280 (*RBR1*), AT1g80080 (*TMM*), and AT5g60880 (*BASL*).

SUPPLEMENTAL INFORMATION

Supplemental Information is available at *Molecular Plant Online*.

FUNDING

This work was supported by grants from the National Natural Science Foundation of China program 31271463 and 31471362 (J.L.), 31071198 and 31471285 (K.Y.), Chinese Academy of Sciences Hundred Talents Program KSCX2-YW-N-073 (J.L.), and a Discovery Grant from the Natural Sciences and Engineering Research Council of Canada (F.S.).

ACKNOWLEDGMENTS

We thank Yan Guo, De Ye, and Dongtao Ren for help in kinase activity assays; De Ye for providing the *LAT52* plasmids; Dominique Bergmann for the seeds of *BASLpro:GFP-BASL*, *SPCHpro:SPCH-GFP*, and *SPCHpro:nucGFP* marker lines; Shuhua Yang for the seeds of *ICE1pro:ICE1-GFP* line and *ice1-1 scrm2-1* double mutants; Tao Wang for the *SPCH-AD* plasmids; Eugenia Russinova for the SPCH plasmids; and Arp Schnittger for the CDK–Cyclin complex plasmids. We thank the anonymous reviewers for suggestions on kinase assay and on mutant naming. No conflict of interest declared.

Received: September 4, 2014
Revised: December 5, 2014
Accepted: December 7, 2014
Published: December 30, 2014

REFERENCES

Beaudette, K.N., Lew, J., and Wang, J.H. (1993). Substrate specificity characterization of a cdc2-like protein kinase purified from bovine brain. J. Biol. Chem. **268**:20825–20830.

Bergmann, D.C., and Sack, F.D. (2007). Stomatal development. Annu. Rev. Plant Biol. **58**:163–181.

Bergmann, D.C., Lukowitz, W., and Somerville, C.R. (2004). Stomatal development and pattern controlled by a MAPKK kinase. Science **304**:1494–1497.

Boudolf, V., Barroco, R., de Almeida Engler, J., Verkest, A., Beeckman, T., Naudts, M., Inze, D., and De Veylder, L. (2004). B1-type cyclin-dependent kinases are essential for the formation of stomatal complexes in *Arabidopsis thaliana*. Plant Cell **16**:945–955.

Casson, S.A., and Hetherington, A.M. (2010). Environmental regulation of stomatal development. Curr. Opin. Plant Biol. **13**:90–95.

Clough, S.J., and Bent, A.F. (1998). Floral dip: a simplified method for *Agrobacterium*-mediated transformation of *Arabidopsis thaliana*. Plant J. **16**:735–743.

Dissmeyer, N., and Schnittger, A. (2011). Use of phospho-site substitutions to analyze the biological relevance of phosphorylation events in regulatory networks. In Plant Kinases, N. Dissmeyer and A. Schnittger, eds. (New York: Humana Press), pp. 93–138.

Dong, J., MacAlister, C.A., and Bergmann, D.C. (2009). BASL controls asymmetric cell division in *Arabidopsis*. Cell **137**:1320–1330.

Gaamouche, T., Manes, C.-L.D.O., Kwiatkowska, D., Berckmans, B., Koumproglou, R., Maes, S., Beeckman, T., Vernoux, T., Doonan, J.H., Traas, J., et al. (2010). Cyclin-dependent kinase activity maintains the shoot apical meristem cells in an undifferentiated state. Plant J. **64**:26–37.

Gudesblat, G.E., Schneider-Pizon, J., Betti, C., Mayerhofer, J., Vanhoutte, I., van Dongen, W., Boeren, S., Zhiponova, M., de Vries, S., Jonak, C., et al. (2012). SPEECHLESS integrates brassinosteroid and stomata signalling pathways. Nat. Cell Biol. **14**:548–554.

Harashima, H., and Schnittger, A. (2012). Robust reconstitution of active cell-cycle control complexes from co-expressed proteins in bacteria. Plant Methods **8**:23.

Harashima, H., Shinmyo, A., and Sekine, M. (2007). Phosphorylation of threonine 161 in plant cyclin-dependent kinase A is required for cell division by activation of its associated kinase. Plant J. **52**:435–448.

Hemerly, A., de Almeida Engler, J., Bergounioux, C., Van Montagu, M., Engler, G., Inze, D., and Ferreira, P. (1995). Dominant negative mutants of the Cdc2 kinase uncouple cell division from iterative plant development. EMBO J. **14**:3925–3936.

Hemerly, A.S., Ferreira, P.C.G., Van Montagu, M., Engler, G., and Inze, D. (2000). Cell division events are essential for embryo patterning and morphogenesis: studies on dominant-negative cdc2aAt mutants of *Arabidopsis*. Plant J. **23**:123–130.

Iwakawa, H., Shinmyo, A., and Sekine, M. (2006). *Arabidopsis* CDKA;1, a cdc2 homologue, controls proliferation of generative cells in male gametogenesis. Plant J. **45**:819–831.

Joubès, J., De Schutter, K., Verkest, A., Inzé, D., and De Veylder, L. (2004). Conditional, recombinase-mediated expression of genes in plant cell cultures. Plant J. **37**:889–896.

Kanaoka, M.M., Pillitteri, L.J., Fujii, H., Yoshida, Y., Bogenschutz, N.L., Takabayashi, J., Zhu, J.-K., and Torii, K.U. (2008). SCREAM/ICE1 and SCREAM2 specify three cell-state transitional steps leading to *Arabidopsis* stomatal differentiation. Plant Cell **20**:1775–1785.

Khan, M., Rozhon, W., Bigeard, J., Pflieger, D., Husar, S., Pitzschke, A., Teige, M., Jonak, C., Hirt, H., and Poppenberger, B. (2013). Brassinosteroid-regulated GSK3/Shaggy-like kinases phosphorylate mitogen-activated protein (MAP) kinase kinases, which control stomata development in *Arabidopsis thaliana*. J. Biol. Chem. **288**:7519–7527.

Kim, T.W., Michniewicz, M., Bergmann, D.C., and Wang, Z.Y. (2012). Brassinosteroid regulates stomatal development by GSK3-mediated inhibition of a MAPK pathway. Nature **482**:419–422.

Lai, L., Nadeau, J.A., Lucas, J., Lee, E.-K., Nakagawa, T., Zhao, L., Geisler, M.J., and Sack, F.D. (2005). The *Arabidopsis* R2R3 MYB proteins FOUR LIPS and MYB88 restrict divisions late in the stomatal cell lineage. Plant Cell **17**:2754–2767.

Lampard, G.R. (2009). The missing link? *Arabidopsis* SPCH is a MAPK specificity factor that controls entry into the stomatal lineage. Plant Signal. Behav. **4**:425–427.

Lampard, G.R., MacAlister, C.A., and Bergmann, D.C. (2008). *Arabidopsis* stomatal initiation is controlled by MAPK-mediated regulation of the bHLH SPEECHLESS. Science **322**:1113–1116.

Lau, O.S., and Bergmann, D.C. (2012). Stomatal development: a plant's perspective on cell polarity, cell fate transitions and intercellular communication. Development **139**:3683–3692.

Le, J., Zou, J.J., Yang, K.Z., and Wang, M. (2014). Signaling to stomatal initiation and cell division. Front. Plant Sci. **5**:297.

Lee, E., Lucas, J.R., and Sack, F.D. (2014). Deep functional redundancy between FAMA and FOUR LIPS in stomatal development. Plant J. **78**:555–565.

MacAlister, C.A., Ohashi-Ito, K., and Bergmann, D.C. (2007). Transcription factor control of asymmetric cell divisions that establish the stomatal lineage. Nature **445**:537–540.

Malamy, J.E., and Benfey, P.N. (1997). Organization and cell differentiation in lateral roots of *Arabidopsis thaliana*. Development **124**:33–44.

Menges, M., De Jager, S.M., Gruissem, W., and Murray, J.A.H. (2005). Global analysis of the core cell cycle regulators of *Arabidopsis* identifies novel genes, reveals multiple and highly specific profiles of expression and provides a coherent model for plant cell cycle control. Plant J. **41**:546–566.

Muschietti, J., Dircks, L., Vancanneyt, G., and McCormick, S. (1994). LAT52 protein is essential for tomato pollen development: pollen expressing antisense LAT52 RNA hydrates and germinates abnormally and cannot achieve fertilization. Plant J. **6**:321–338.

Nadeau, J.A. (2009). Stomatal development: new signals and fate determinants. Curr. Opin. Plant Biol. **12**:29–35.

Nadeau, J.A., and Sack, F.D. (2002a). Stomatal development in *Arabidopsis*. In Arabidopsis Book, C.R. Somerville and E.M. Meyerowitz, eds. (Rockville, MD: American Society of Plant Biologists) **1**:e0066.

Nadeau, J.A., and Sack, F.D. (2002b). Control of stomatal distribution on the *Arabidopsis* leaf surface. Science **296**:1697–1700.

Nowack, M.K., Grini, P.E., Jakoby, M.J., Lafos, M., Koncz, C., and Schnittger, A. (2006). A positive signal from the fertilization of the egg cell sets off endosperm proliferation in angiosperm embryogenesis. Nat. Genet. **38**:63–67.

Nowack, M.K., Harashima, H., Dissmeyer, N., Zhao, X.A., Bouyer, D., Weimer, A.K., De Winter, F., Yang, F., and Schnittger, A. (2012). Genetic framework of cyclin-dependent kinase function in *Arabidopsis*. Dev. Cell **22**:1030–1040.

Oakley, G.G., and Patrick, S.M. (2012). Replication protein A: directing traffic at the intersection of replication and repair. Front. Biosci. (Landmark Ed.) **15**:883–900.

Ohashi-Ito, K., and Bergmann, D.C. (2006). *Arabidopsis* FAMA controls the final proliferation/differentiation switch during stomatal development. Plant Cell **18**:2493–2505.

Pillitteri, L.J., Sloan, D.B., Bogenschutz, N.L., and Torii, K.U. (2007). Termination of asymmetric cell division and differentiation of stomata. Nature **445**:501–505.

Qian, P., Han, B., Forestier, E., Hu, Z., Gao, N., Lu, W., Schaller, H., Li, J., and Hou, S. (2013). Sterols are required for cell-fate commitment and maintenance of the stomatal lineage in *Arabidopsis*. Plant J. **74**:1029–1044.

Walter, M., Chaban, C., Schutze, K., Batistic, O., Weckermann, K., Nake, C., Blazevic, D., Grefen, C., Schumacher, K., Oecking, C., et al. (2004). Visualization of protein interactions in living plant cells using bimolecular fluorescence complementation. Plant J. **40**:428–438.

Wang, H., Ngwenyama, N., Liu, Y., Walker, J.C., and Zhang, S. (2007). Stomatal development and patterning are regulated by environmentally responsive mitogen-activated protein kinases in *Arabidopsis*. Plant Cell **19**:63–73.

Wang, M., Yang, K.Z., and Le, J. (2014). Organ-specific effects of brassinosteroids on stomatal production coordinate with the action of TOO MANY MOUTHS. J. Integr. Plant Biol. http://dx.doi.org/10.1111/jipb.12285.

Weimer, A.K., Nowack, M.K., Bouyer, D., Zhao, X., Harashima, H., Naseer, S., De Winter, F., Dissmeyer, N., Geldner, N., and Schnittger, A. (2012). Retinoblastoma related1 regulates asymmetric cell divisions in *Arabidopsis*. Plant Cell **24**:4083–4095.

Wengier, D.L., and Bergmann, D.C. (2012). On fate and flexibility in stomatal development. Cold Spring Harb. Symp. Quant. Biol. **77**:53–62.

Xie, Z., Lee, E., Lucas, J.R., Morohashi, K., Li, D., Murray, J.A.H., Sack, F.D., and Grotewold, E. (2010). Regulation of cell proliferation in the stomatal lineage by the *Arabidopsis* MYB FOUR LIPS via direct targeting of core cell cycle genes. Plant Cell **22**:2306–2321.

Yang, K., Wang, H., Xue, S., Qu, X., Zou, J., and Le, J. (2014). Requirement for A-type cyclin-dependent kinase and cyclins for the terminal division in the stomatal lineage of *Arabidopsis*. J. Exp. Bot. **65**:2449–2461.